

This supplementary information was updated on 20<sup>th</sup> May 2020.

**RGD functionalized chitosan nanoparticle mediated targeted delivery of raloxifene selectively suppresses angiogenesis and tumor growth in breast cancer**

This supplementary information has been updated to reflect the following changes:

- Incorrect affiliation information for the authorship list has been corrected
- In Figure S7, panel 'a', "10 $\mu$ M" should be labelled above Rlx and Rlx-CHNP only. Figure legend of S7, panel 'a' has been modified accordingly.
- In Figure S9(a), the uppermost panel inadvertently displayed the incorrect images. This has been corrected in the new version.

The original versions of Figure S7 and Figure S9, along with their original captions, have been copied below for future reference.

Please contact [Nanoscale@rsc.org](mailto:Nanoscale@rsc.org) with any inquiries, citing the DOI: doi.org/10.1039/C9NR10673A

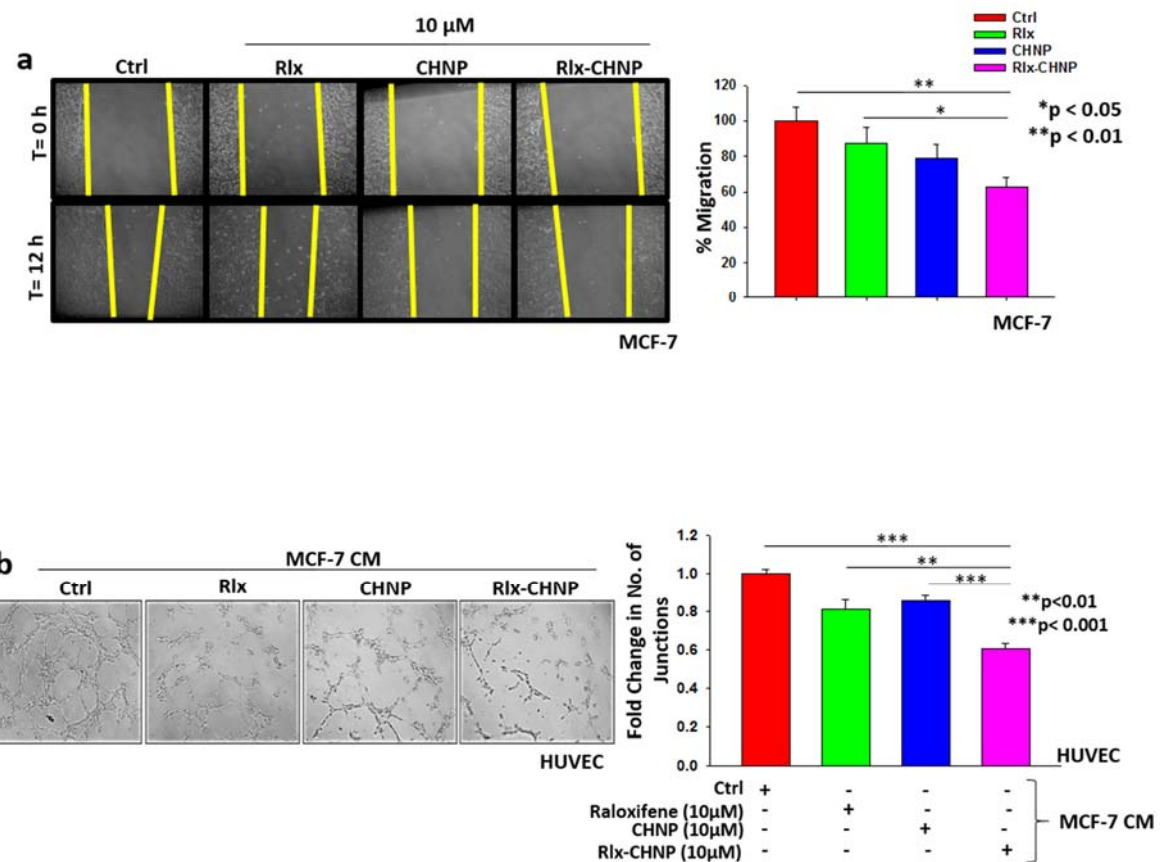


**Figure S7.** Rlx-CHNPs inhibited MCF-7 cell migration and angiogenesis **(a)** Confluent monolayer of MCF-7 cells were wounded with constant width and treated with 10  $\mu$ M of free Rlx, CHNP and Rlx-CHNP in 2.5% serum condition for 12 h at pH 6.5, photographs of wound were taken at  $t = 0$  h and  $t = 12$  h. Area migrated was analyzed by using image-Pro plus software and represented in the form of bar graph (mean  $\pm$  SEM,  $n = 3$  independent experiments). **(b)** HUVEC (1x10<sup>4</sup>) were seeded on Matrigel-coated plate and then supplemented with CM of MCF-7 cells either treated with free Rlx, CHNP or Rlx-CHNP (10  $\mu$ M each). CM of untreated cells was used as control. After 6 h of incubation, endothelial cell tubular structure formation was photographed and analyzed. Number of junctions were measured by using AngioTool64 0.6a software and represented as fold change compared to control in the form of bar graph (mean  $\pm$  SEM,  $n = 3$  independent experiments; \* $p < 0.05$ , \*\* $p < 0.01$  and \*\*\* $p < 0.001$  ).

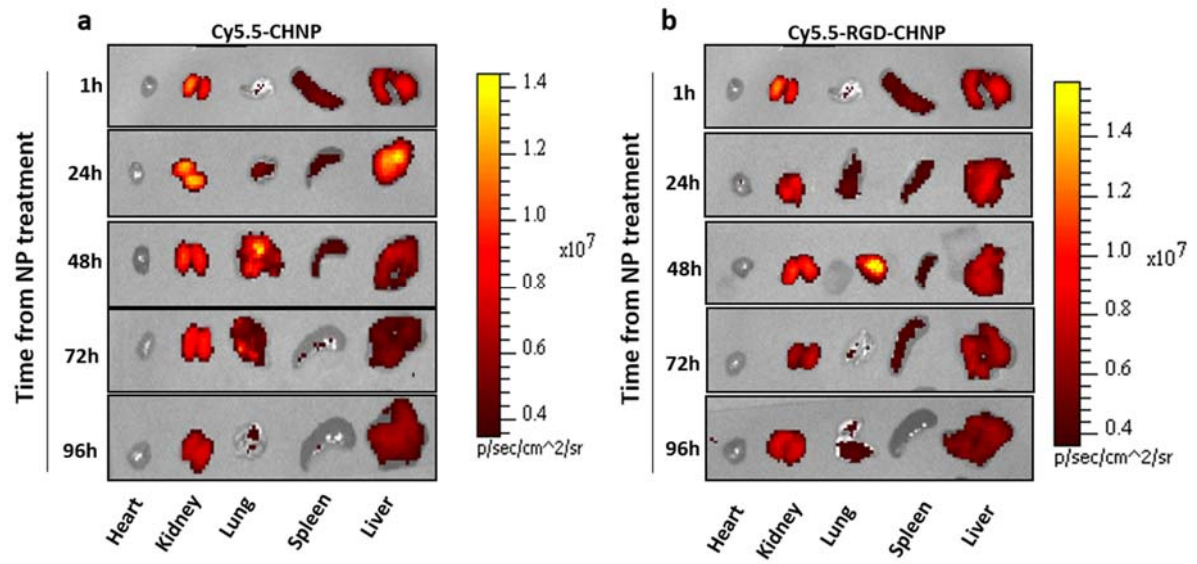


**Figure S9.** NIRF images captured by ex vivo imaging of major organs dissected from (a) Cy5.5-CHNP and (b) Cy5.5-RGD-CHNP treated mice at various time points.

# RGD functionalized chitosan nanoparticle mediated targeted delivery of raloxifene selectively suppresses angiogenesis and tumor growth in breast cancer

Amit S. Yadav,<sup>‡,a</sup> N Naga Venkata Radharani,<sup>‡,a</sup> Mahadeo Gorain,<sup>a</sup> Anuradha Bulbule,<sup>a</sup> Dattatrya Shetti,<sup>§,a</sup> Gaurab Roy,<sup>§,a</sup> Thejus Baby,<sup>¶,a</sup> and Gopal C. Kundu<sup>\*a,b</sup>

<sup>a</sup>Laboratory of Tumor Biology, Angiogenesis and Nanomedicine Research, National Centre for Cell Science (NCCS), Pune 411007, India. E-mail: [yadav.singh.amit@gmail.com](mailto:yadav.singh.amit@gmail.com); [radha.smile08@gmail.com](mailto:radha.smile08@gmail.com); [mahadeo.gorain@gmail.com](mailto:mahadeo.gorain@gmail.com); [anuradha@nccs.res.in](mailto:anuradha@nccs.res.in); [dattakapilshetti@gmail.com](mailto:dattakapilshetti@gmail.com); [groy86@hotmail.com](mailto:groy86@hotmail.com); [baby.thejuss@gmail.com](mailto:baby.thejuss@gmail.com)

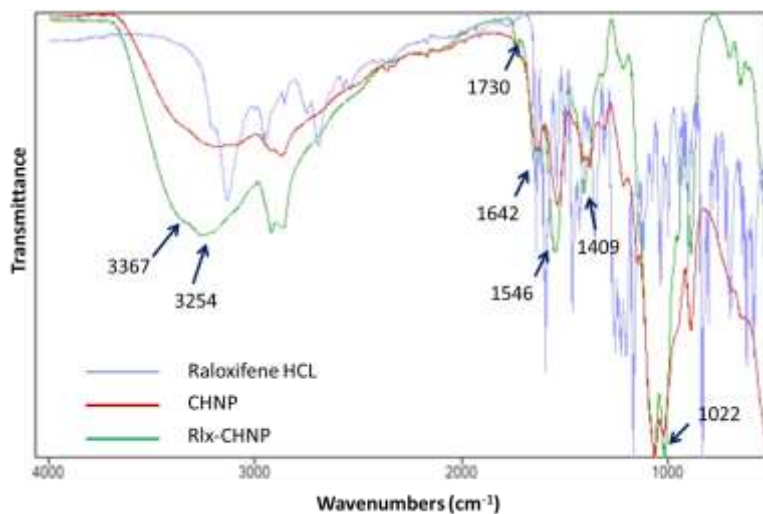
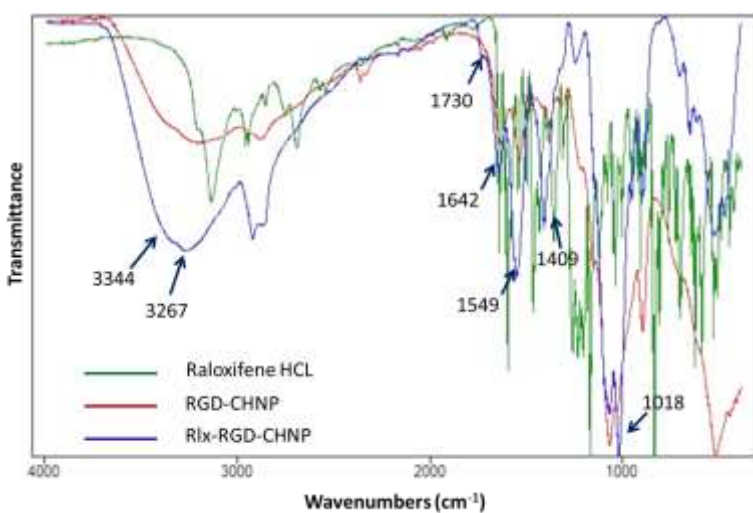
<sup>§</sup>Present address: School of Biology and Biological Engineering, South China University of Technology, Guangzhou 510006, China

<sup>¶</sup>Present address: Australian Institute for Bioengineering and Nanotechnology, University of Queensland, St.Lucia QLD 4072, Australia.

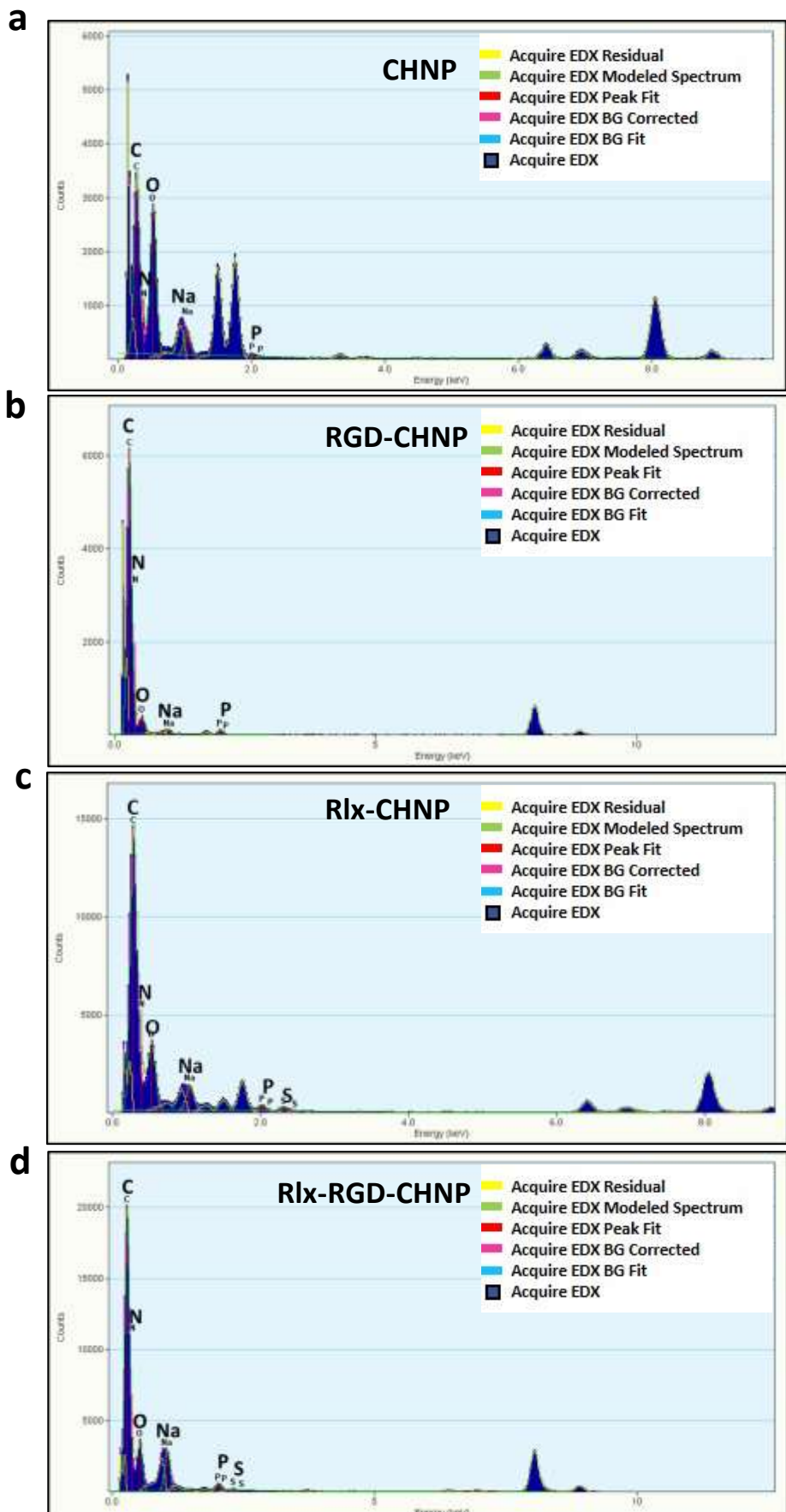
<sup>b</sup>School of Biotechnology and Kalinga Institute of Medical Sciences (KIMS), KIIT Deemed to be University, Institute of Eminence, Bhubaneswar 751024, India. E-mail: [gopalc.kundu@kiit.ac.in](mailto:gopalc.kundu@kiit.ac.in)

<sup>‡</sup>These authors contributed equally.

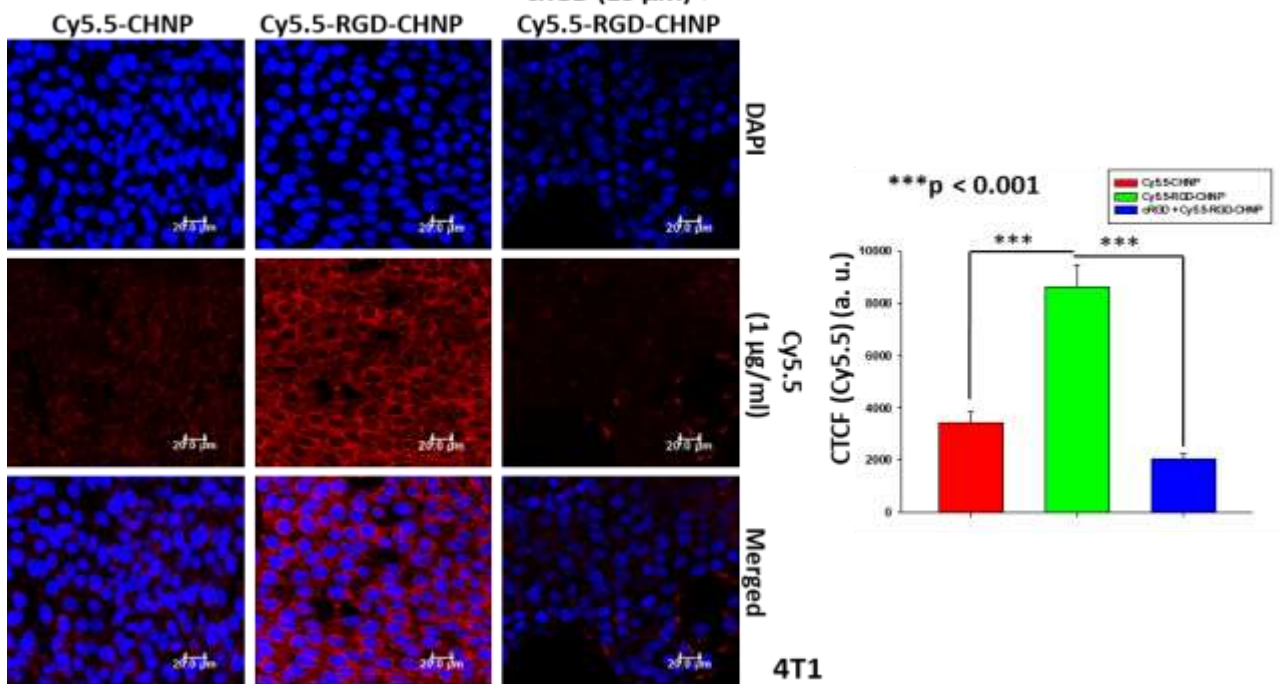
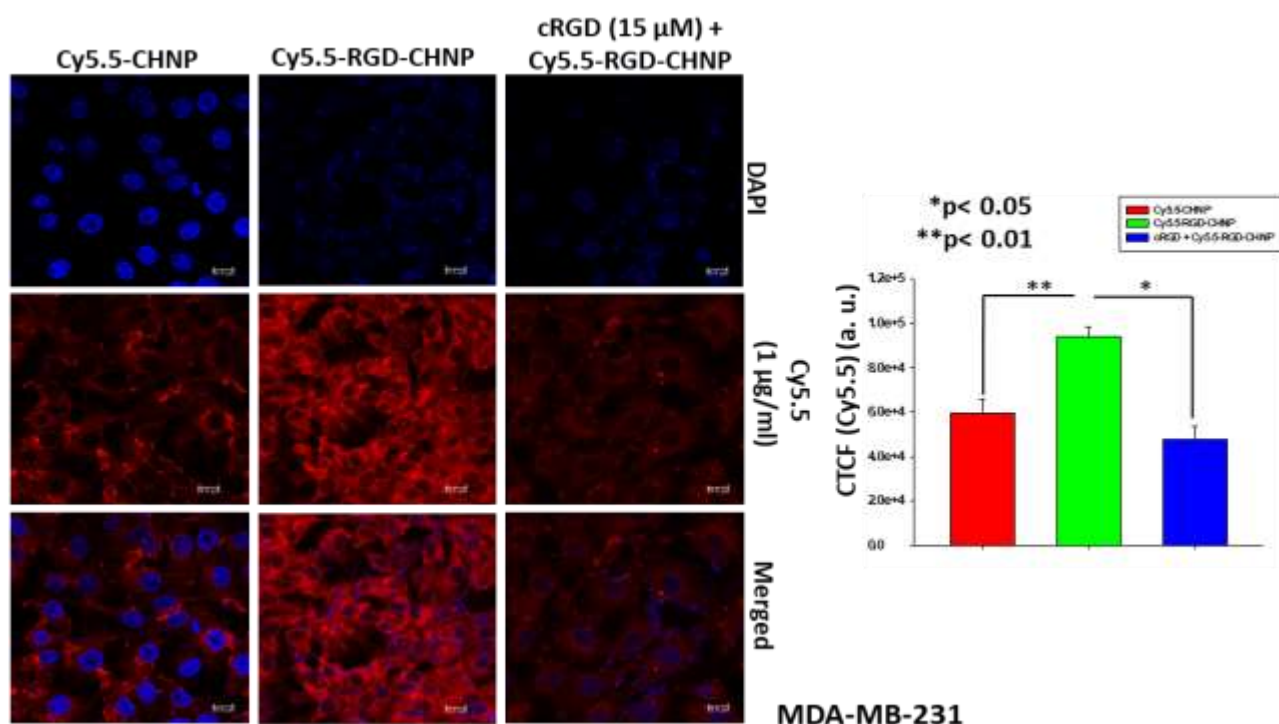
\*Correspondence.

**a****b**

**Figure S1.** FTIR spectra of (a) Raloxifene, CHNP, Rlx-CHNP; (b) Raloxifene, RGD-CHNP, and Rlx-RGD-CHNP



**Figure S2.** TEM-EDX analysis of (a) CHNP, (b) RGD-CHNP, (c) Rlx-CHNP and (d) Rlx-RGD-CHNP

**a****b**

**Figure S3. Enhanced cellular uptake of RGD-CHNPs in  $\alpha_v\beta_3$  integrin expressing breast cancer cells is mediated by RGD peptide.** Laser confocal microscopic images of (a) 4T1 and (b) MDA-MB-231 cells incubated with Cy5.5-CHNPs or Cy5.5-RGD-CHNP (1  $\mu$ g/ml of Cy5.5) for 2 h or treated with cRGDfK (15  $\mu$ M) for 30 min prior to Cy5.5-RGD-CHNP treatment. Corrected total cell fluorescence (CTCF) of Cy5.5 was quantified from the images by NIH ImageJ software (ImageJ Freeware; <http://rsb.info.nih.gov/ij/>) and represented in the form of bar graph (mean  $\pm$  SE; \*p < 0.05, \*\*p < 0.01 and \*\*\*p < 0.001).

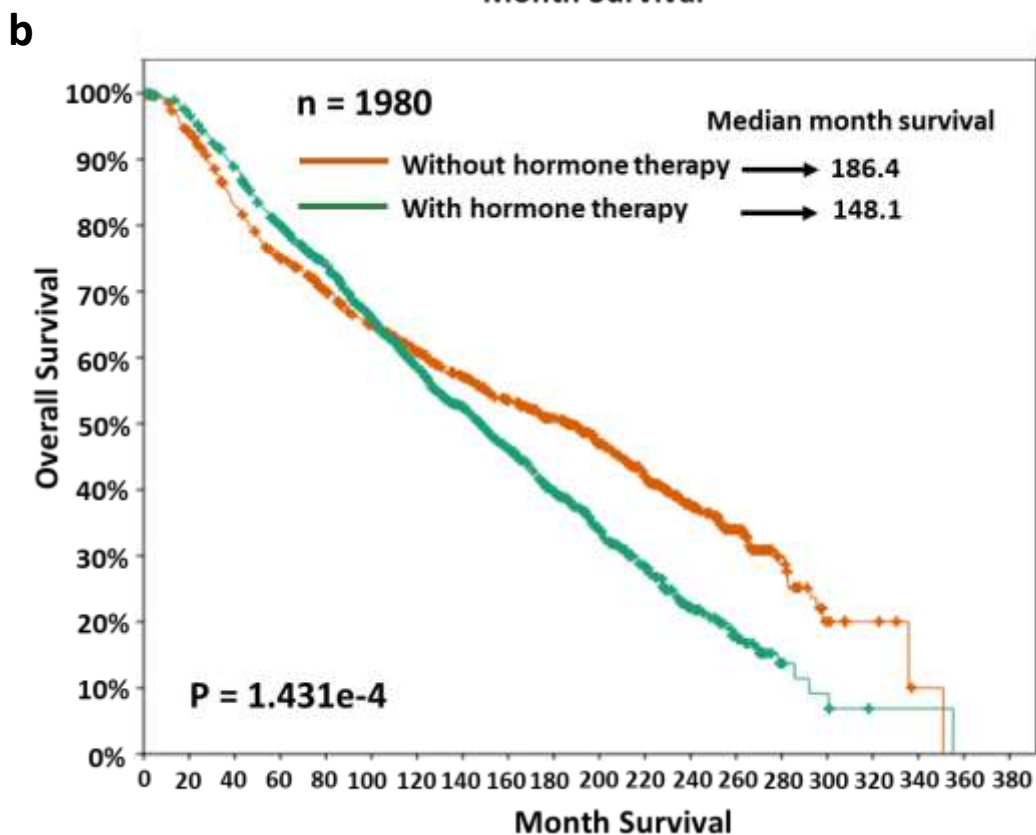
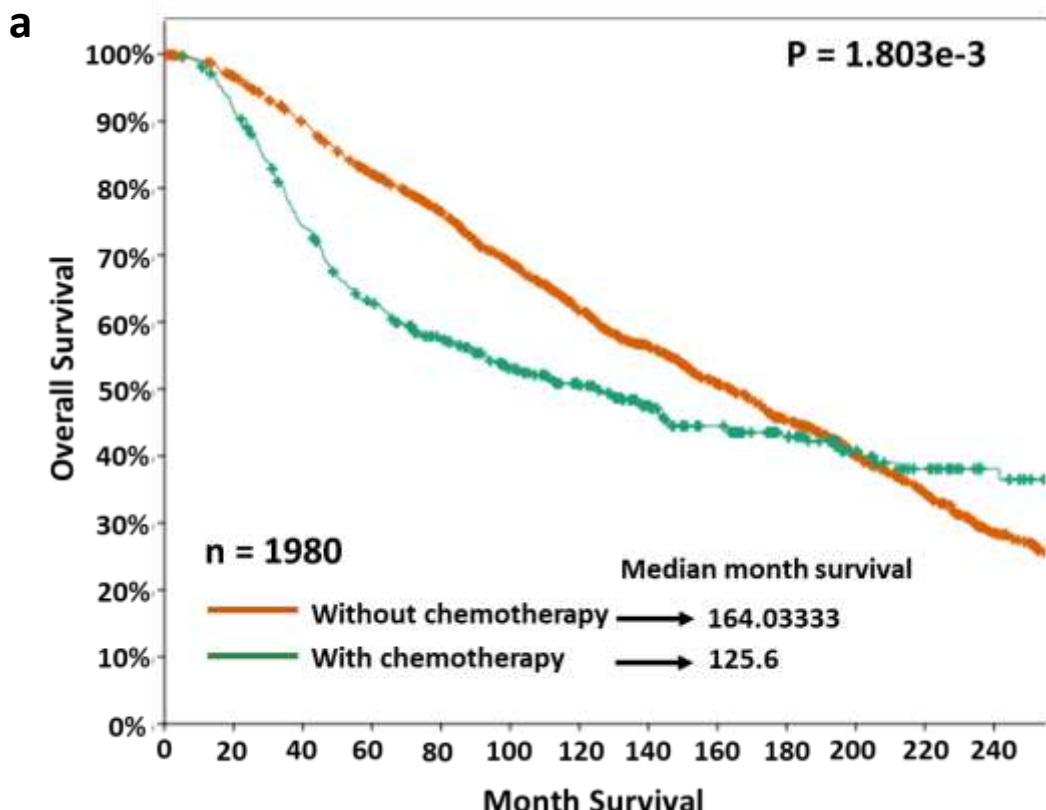


**Figure S4.** The integrated Kaplan-Meier plots obtained from TCGA cohorts representing overall survival in **(a)** patients with and without chemotherapy **(b)** patients with and without hormone therapy.

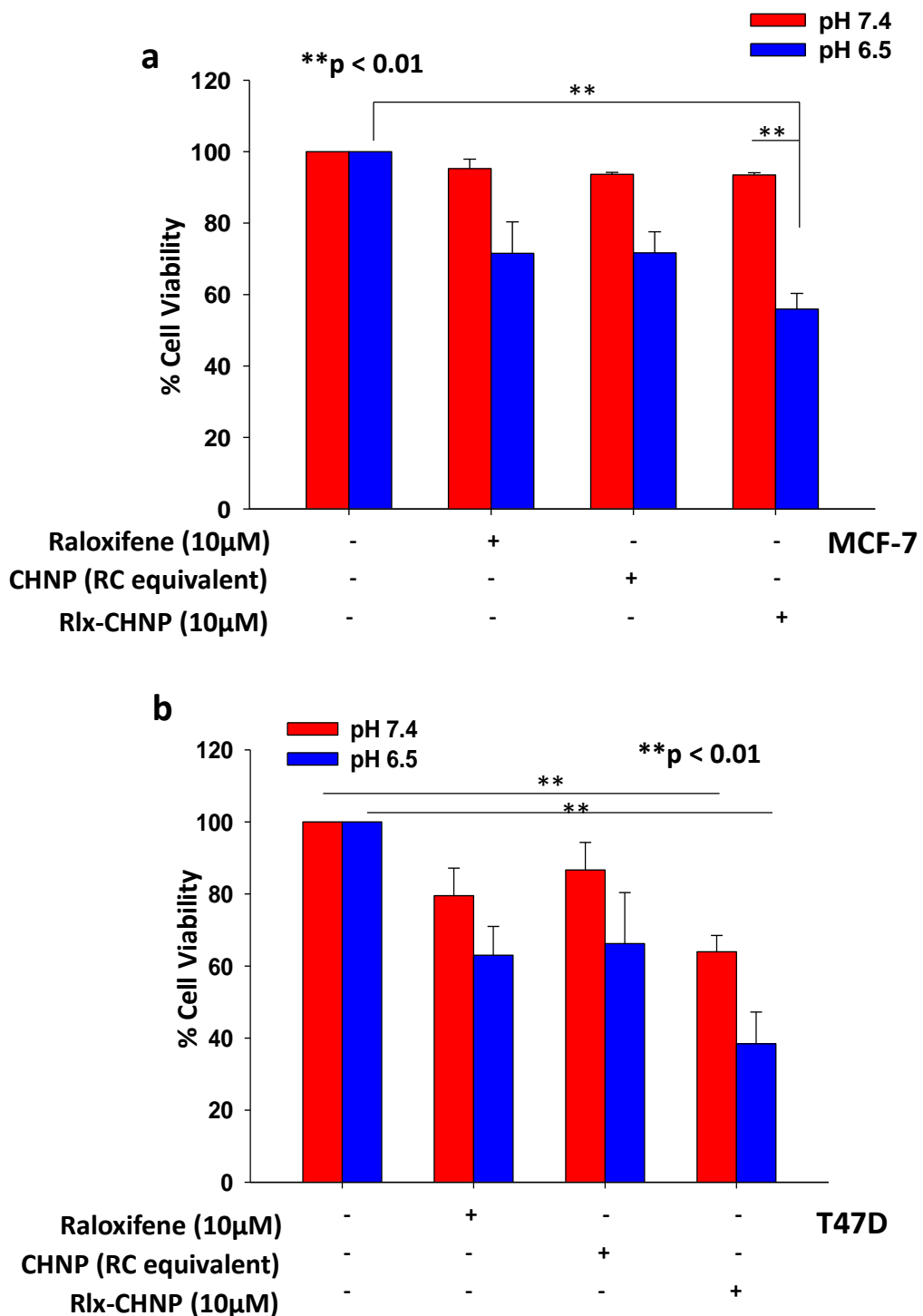


**Figure S5.** Cytotoxicity of Rlx, CHNP and Rlx-CHNP against **(a)** MCF-7 and **(b)** T47D cells was analyzed by MTT assay as a function of Rlx-equivalent concentration (10  $\mu$ M) at pH 7.4 and 6.5 respectively. Rlx loaded CHNP showed higher efficacy at low pH compared to other treatments. Error bars represent mean  $\pm$  SEM, n=3 independent experiments; \*\*p < 0.01.

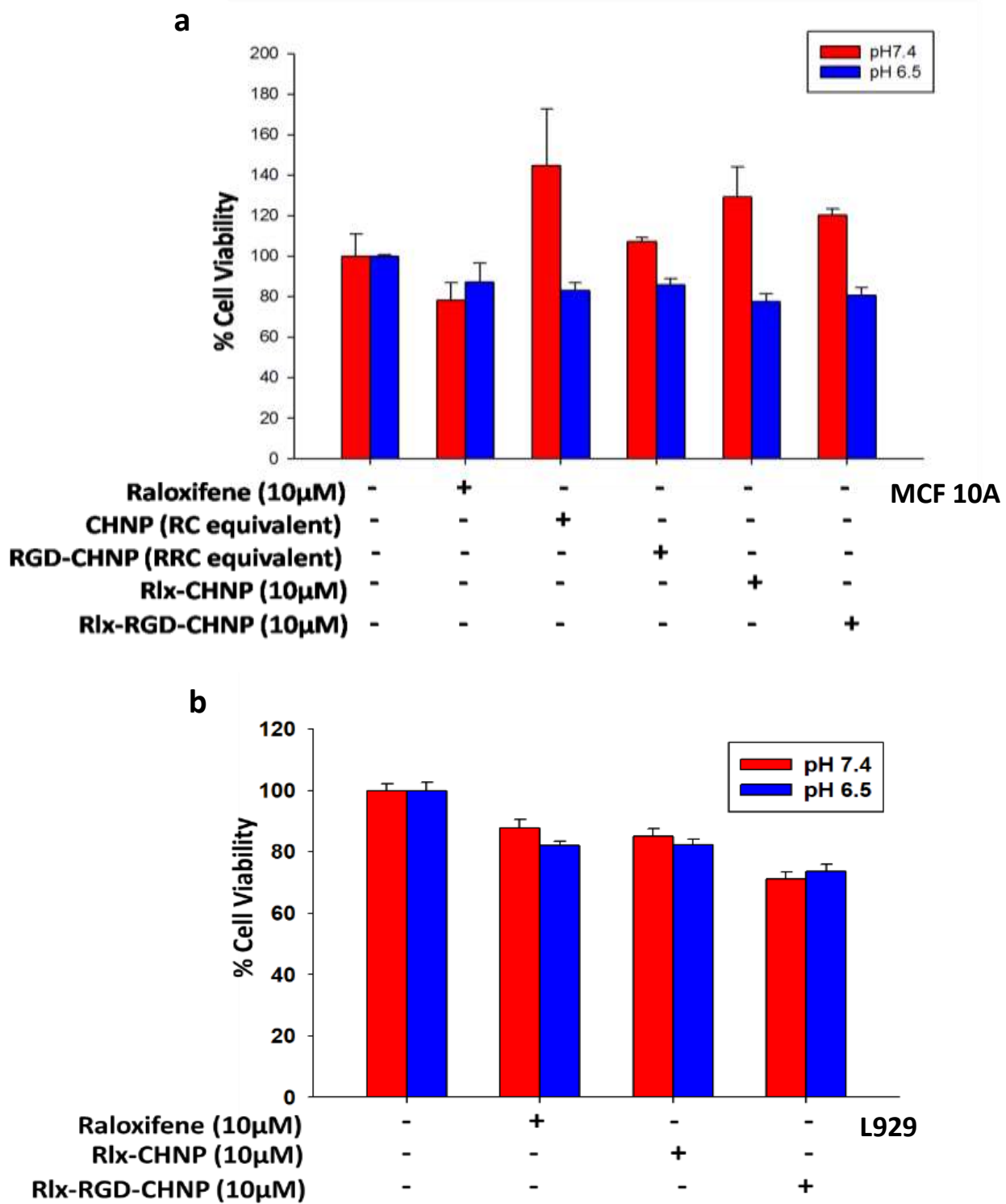


**Figure S6.** Cytotoxicity of NPs in **(a)** MCF 10A and **(b)** L929 cells was analyzed as a function of Rlx-equivalent concentration (10  $\mu$ M). Briefly, cells were treated with free Rlx and NPs (10  $\mu$ M) for 24 hrs at pH 7.4 and 6.5 respectively and MTT assay was performed.

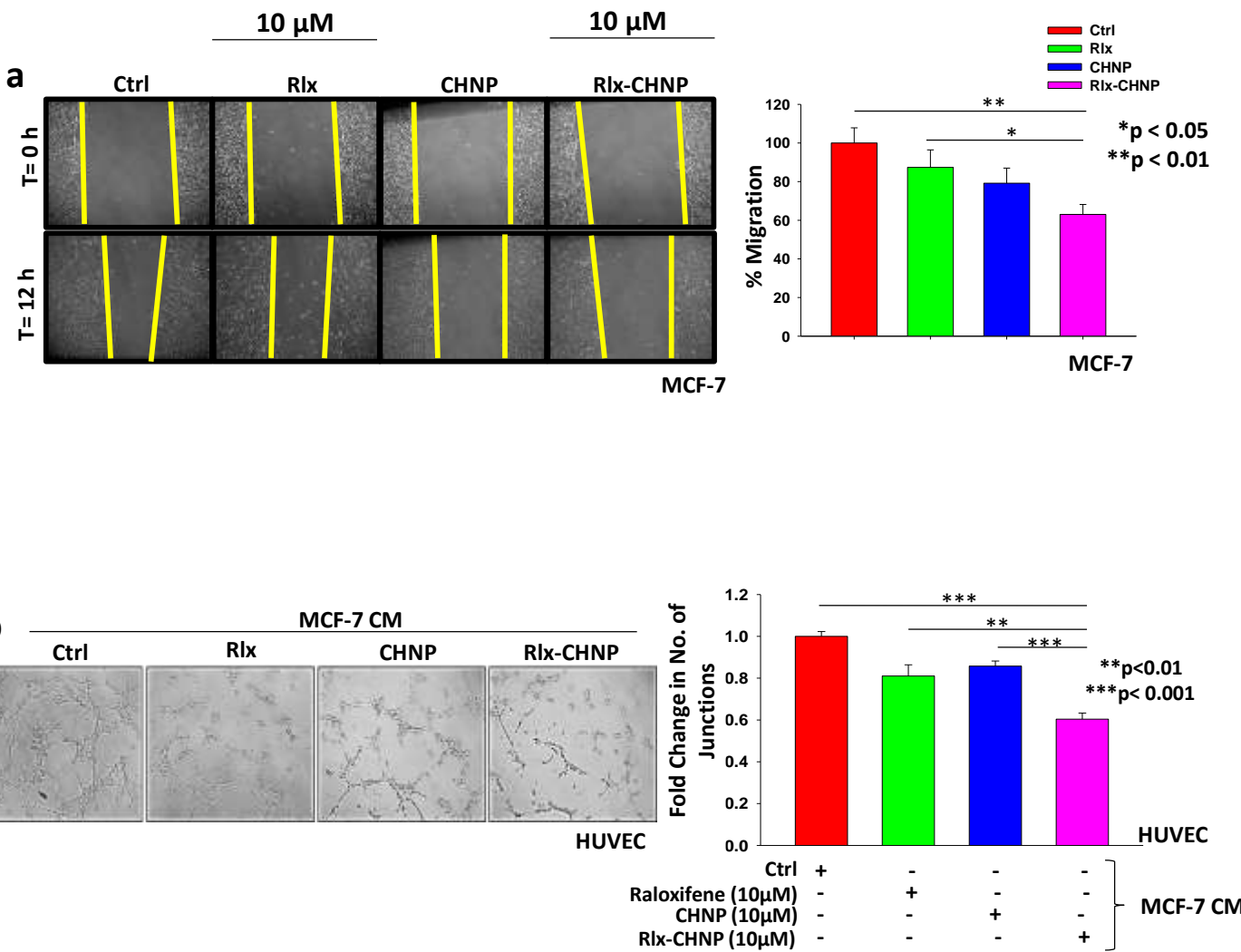


**Figure S7.** Rlx-CHNPs inhibited MCF-7 cell migration and angiogenesis **(a)** Confluent monolayer of MCF-7 cells were wounded with constant width and treated with free Rlx, CHNP and Rlx-CHNP in 2.5% serum condition for 12 h at pH 6.5, photographs of wound were taken at  $t = 0$  h and  $t = 12$  h. Area migrated was analyzed by using image-Pro plus software and represented in the form of bar graph (mean  $\pm$  SEM,  $n = 3$  independent experiments). **(b)** HUVEC ( $1 \times 10^4$ ) were seeded on Matrigel-coated plate and then supplemented with CM of MCF-7 cells either treated with free Rlx, CHNP or Rlx-CHNP. CM of untreated cells was used as control. After 6 h of incubation, endothelial cell tubular structure formation was photographed and analyzed. Number of junctions were measured by using AngioTool64 0.6a software and represented as fold change compared to control in the form of bar graph (mean  $\pm$  SEM,  $n = 3$  independent experiments;  $*p < 0.05$ ,  $**p < 0.01$  and  $***p < 0.001$  ).

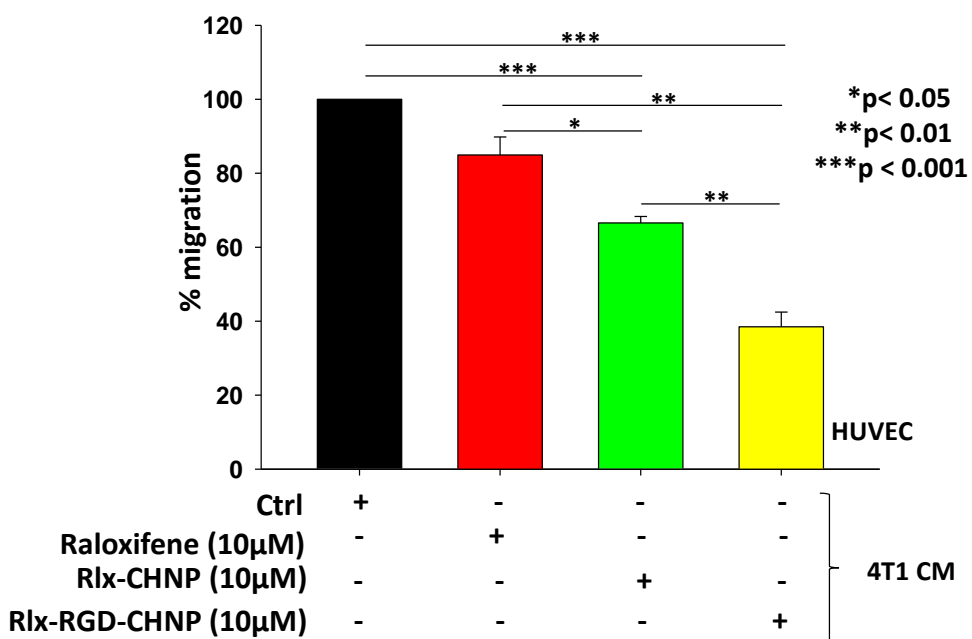
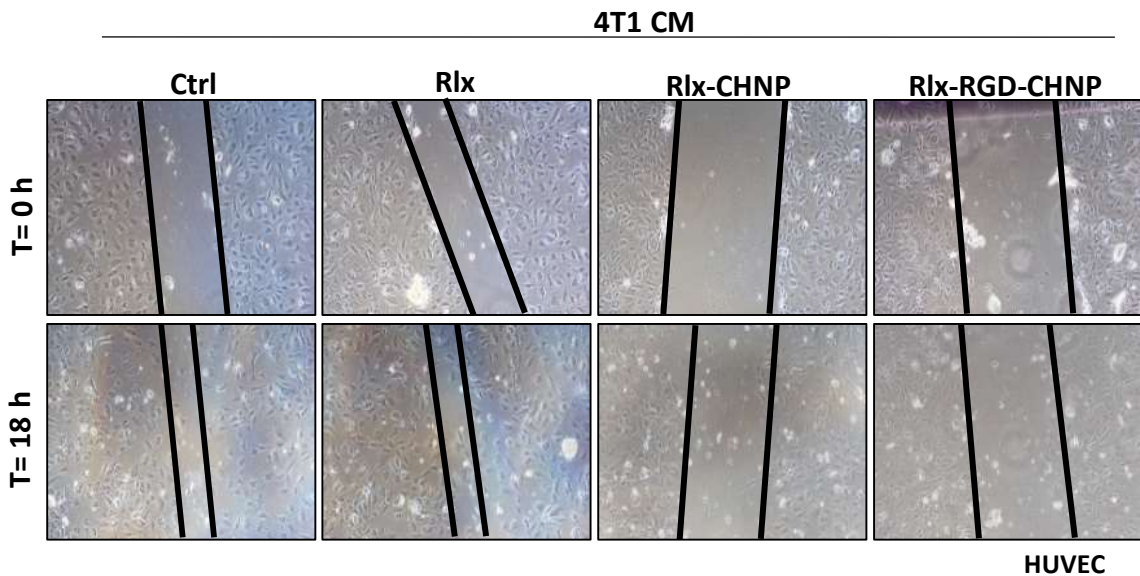


**Figure S8. Rlx-RGD-CHNPs significantly inhibited breast cancer cells (4T1) CM induced endothelial cell migration.** Confluent monolayer of HUVECs were wounded with constant width and then supplemented with CM of 4T1 cells either treated with free Rlx, Rlx-CHNP or Rlx-RGD-CHNP (10  $\mu$ M each). CM of untreated cells were used as control. Photographs of wound were taken at  $t = 0$  h and  $t = 18$  h. Area migrated was analyzed by using image-Pro plus software and represented in the form of bar graph. The error bar represents mean  $\pm$  SEM,  $n=3$  independent experiments;  $*p < 0.05$ ,  $**p < 0.01$  and  $***p < 0.001$ .

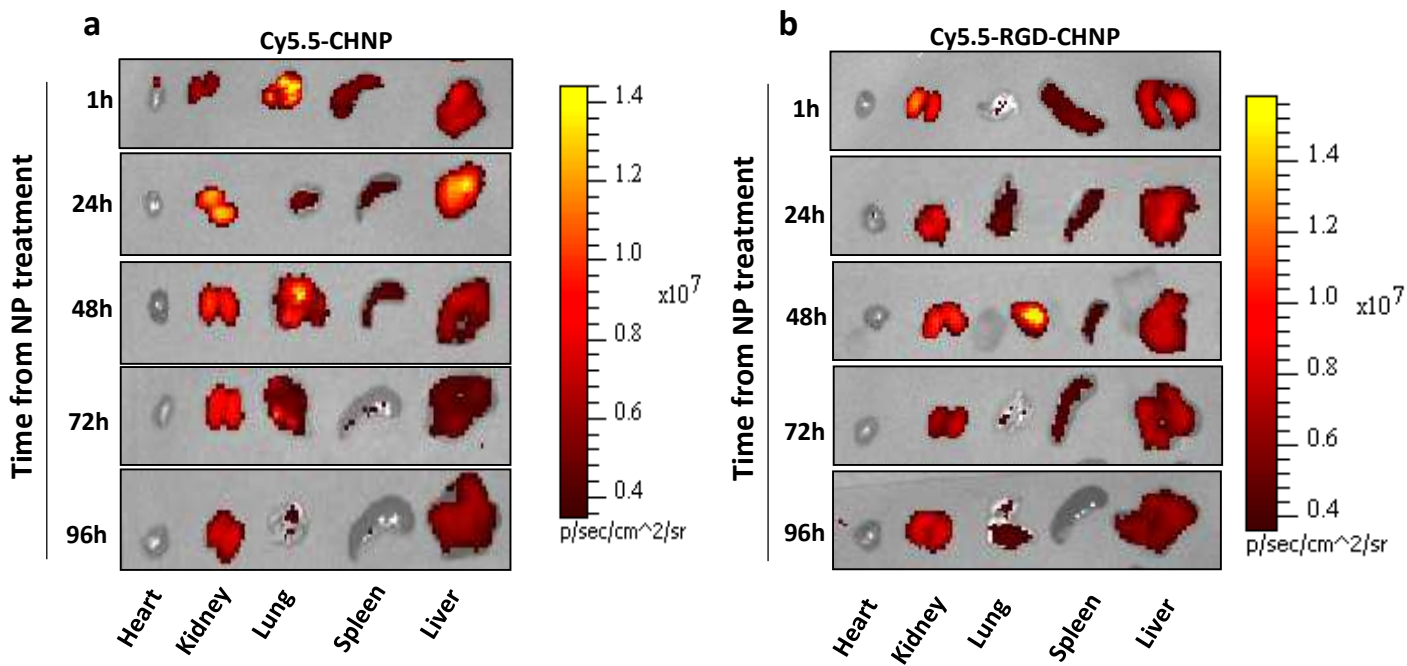


**Figure S9.** NIRF images captured by *ex vivo* imaging of major organs dissected from (a) Cy5.5-CHNP and (b) Cy5.5-RGD-CHNP treated mice at various time points.

10 mg/kg

a

Ctrl

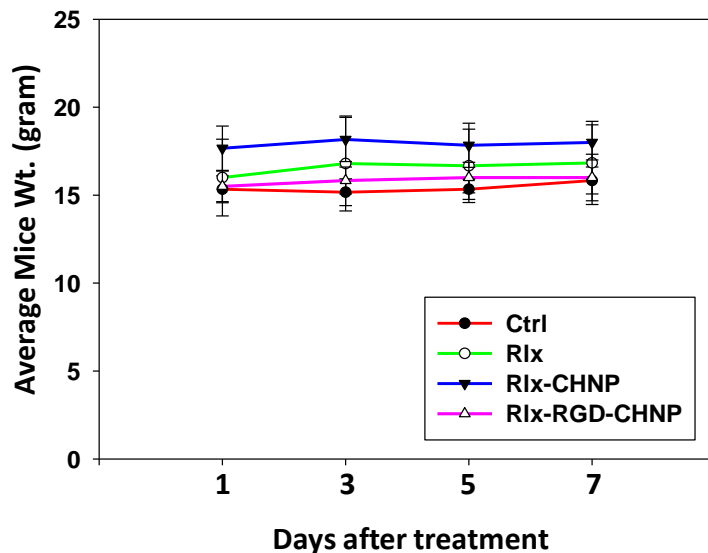
Rlx

Rlx-CHNP

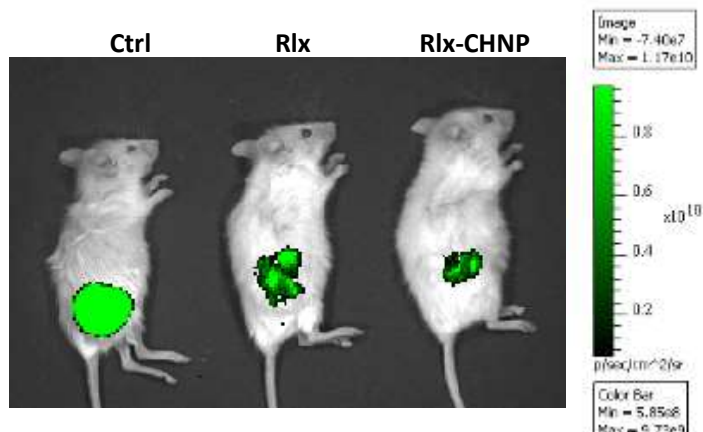
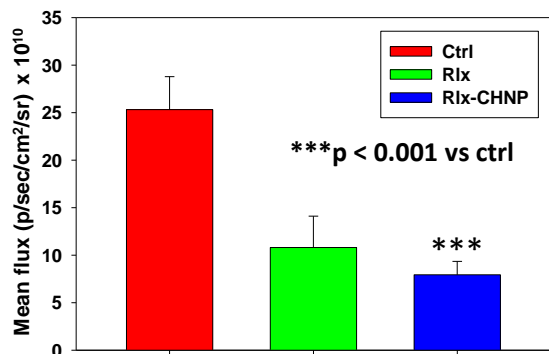
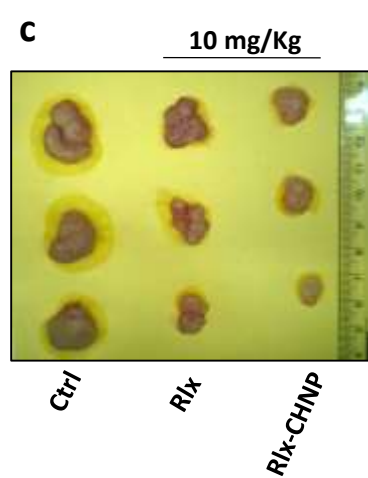
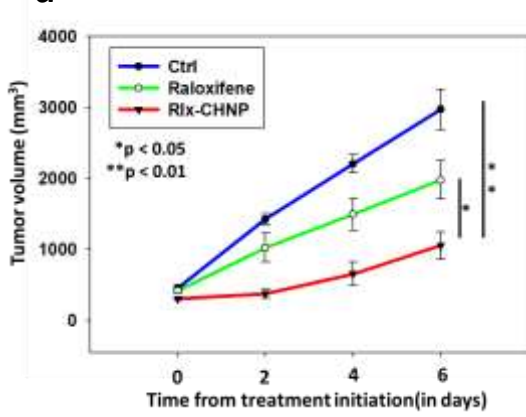
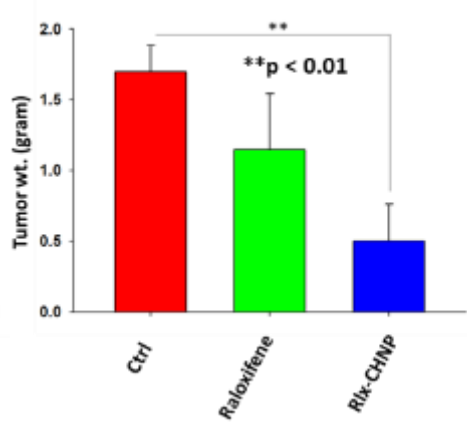
Rlx-RGD-CHNP



b



**Figure S10.** (a) Photographs of representative tumor bearing Balb/c mice. (b) Change in average body weight of 4T1 tumor bearing mice treated with free Rlx, Rlx-CHNP and Rlx-RGD-CHNP as compared to control.

**a****b****c****d****e**

**Figure S11.** Rlx-CHNPs inhibited MCF-7 breast tumor growth in orthotopic NOD/SCID mice model. **(a)** Photographs of fluorescence imaging of representative tumor bearing NOS/SCID mice. **(b)** The bar graph depicts the size of tumors in terms of mean flux (photons/sec/cm<sup>2</sup>/sr)  $\pm$  SE (n=3). **(c)** External appearance of excised tumors. **(d)** Line graph depicts the tumor growth in terms of mean tumor volume  $\pm$  SEM (n=3). **(e)** Excised tumors were weighed and analyzed statistically. Bar graph represents mean tumor weight  $\pm$  SD, n=3; ; \*p < 0.05, \*\*p < 0.01 and \*\*\*p < 0.001.

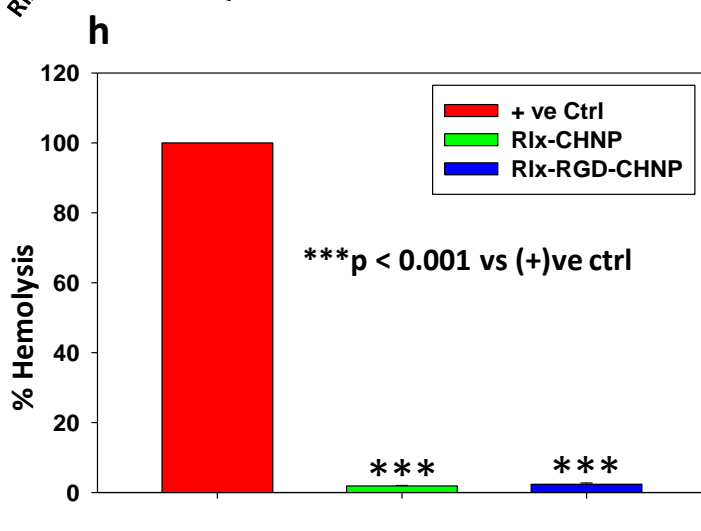
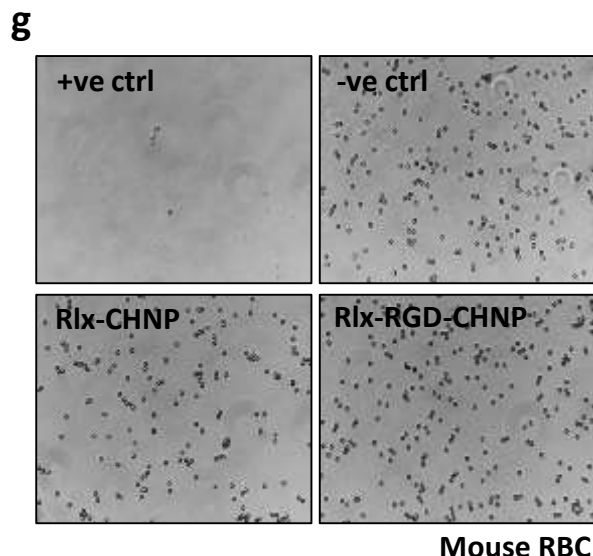
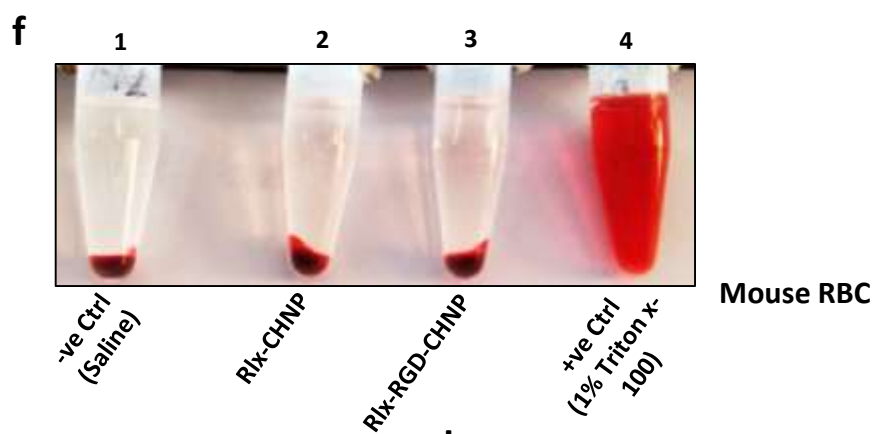
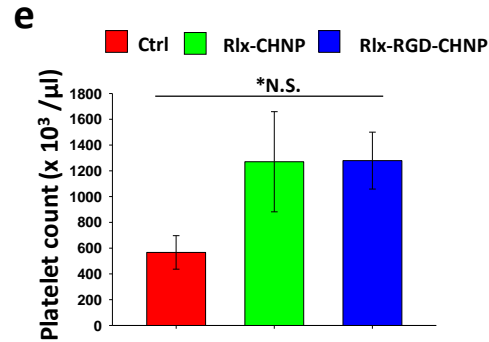
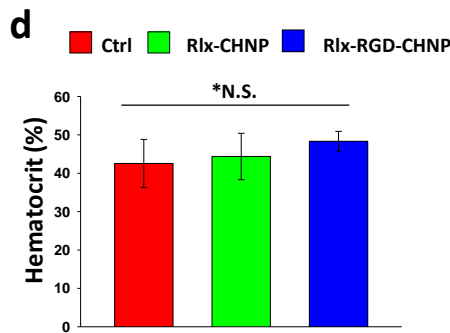
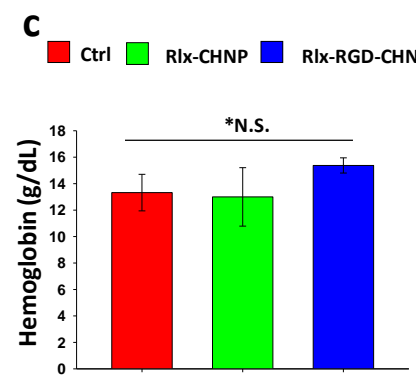
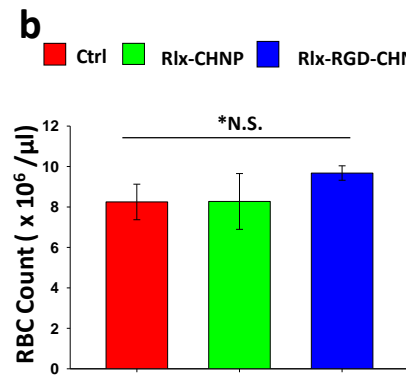
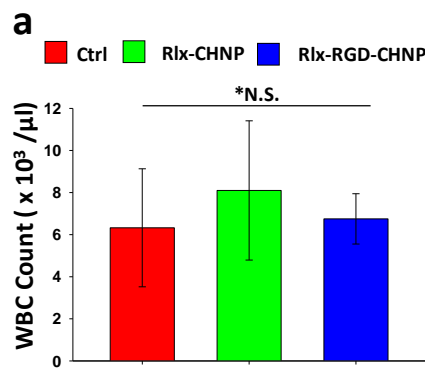


**Figure S12.** Rlx-CHNP and Rlx-RGD-CHNP possess high hemocompatibility. Hematology results of the Rlx-CHNP and Rlx-RGD-CHNP (20 mg/kg body wt) treated female Balb/c mice. **(a)** WBC count, **(b)** RBC count, **(c)** hemoglobin (HGB), **(d)** hematocrit (HCT) and **(e)** platelets count. Bars represent means  $\pm$  standard deviation (n=4, \*N.S. = Not significant). **(f)** Photographs of RBC pallets after exposure with saline, Rlx-CHNP, Rlx-RGD-CHNP and 1% Triton X-100 showing hemolytic activity of NPs. **(g)** Phage contrast images representing morphology of RBCs after exposure with saline, Rlx-CHNP, Rlx-RGD-CHNP and 1% Triton X-100. **(h)** Percentage of hemolysis measured by a spectrophotometer  $\pm$  SEM, n=3; \*\*\*p < 0.001 vs +ve control.